International Journal of Mechanical, Industrial and Aerospace Sciences
ISSN: 2517-9950
Vol:7, No:10, 2013

Investigation on Nanoparticle Velocity in Two Phase Approach

E. Mat Tokit, Yusoff M. Z, Mohammed H.

***Abstract*—**Numerical investigation on the generality of nanoparticle velocity equation had been done on the previous published work. The three dimensional governing equations (continuity, momentum and energy) were solved using finite volume method (FVM). Parametric study of thermal performance between pure water-cooled and nanofluid-cooled are evaluated for volume fraction in the range of 1% to 4%, and nanofluid type of gamma-Al_2O_3 at Reynolds number range of 67.41 to 286.77. The nanofluid is modeled using single and two phase approach. Three different existing Brownian motion velocities are applied in comparing the generality of the equation for a wide parametric condition. Deviation in between the Brownian motion velocity is identified to be due to the different means of mean free path and constant value used in diffusion equation.

***Keywords*—**Brownian nanoparticle velocity, heat transfer enhancement, nanofluid, two phase model.

NOMENCLATURE

c_p specific heat, J/kgK
d_p particle diameter, nm
D diffusion coefficient
D_h hydraulic diameter, mm
De Dean number, $De = Re(D_h/R_c)^{0.5}$
h heat transfer coefficient,
k thermal conductivity, W/mK
M Molecular weight of water, kg/kgmol
N Avogadro number of water
Nu Nusselt number, $Nu = hD_h/k$
Po Poiseuille number, $Po = fRe$
q'' heat flux, kW/cm^2
R radius, nm
R_c curvature radius, mm
Re Reynolds Number, $Re = v\rho D_h/\mu$
R_{th} Thermal resistance, ^oC/ W, $R_{th} = \Delta T/Q$
T temperature, ^oC
u, v, w Velocity component, m/s
x,y, z Cartesian coordinate

Greek symbols
β thermal expansion, 1/K
ρ density, kg/m^3
κ_B Boltzman constant
$\varnothing$ solid volume fraction
μ viscosity, Ns/m^2
λ curvature ratio, $\lambda = D_h/R_c$

Subscripts
f fluid
nf nanofluid
np nanoparticle
pw pure water
rms root mean square
s solid

E. Mat Tokit is with the Faculty of Mechanical Engineering, Universiti Teknikal Malaysia Melaka, Hang Tuah Jaya, 76100 Durian Tunggal, Melaka, Malaysia (phone: 606-2332430; fax: 606-2332429 e-mail: ernie@utem.edu.my).

Yusoff M. Z is with the Department of Mechanical Engineering, College of Engineering, Universiti Tenaga Nasional, Jalan IKRAM-UNITEN, 43000 Kajang, Selangor, Malaysia (e-mail: zamri@uniten.edu.my).

Mohammed H. is with the Department of Thermofluids, Faculty of Mechanical Engineering, Universiti Teknologi Malaysia, 81310 UTM, Skudai, Johor Bahru, Malaysia (e-mail: Hussein.dash@yahoo.com).

I. INTRODUCTION

NANOFLUID, a mixture with novel property is an engineered suspension of nanoparticles in a base fluid. Most researchers modeled the nanofluid as single-phase model and many works have shown the wide application using two-phase approach (mixture and Eulerian) while also other works used porous medium to treat the nanofluid in fluid system

Some studies compared the fluid and thermal analysis of nanofluid using single-phase and two-phase model. Very small deviations of heat transfer coefficient were predicted while overprediction in the enhancement of heat transfer coefficient [1], [2] at higher nanoparticle volume fraction as two-phase model is applied. Meanwhile, the predicted average Nu number was increased monotonously while single-phase model showed linear increment for higher particle concentration [2]. The Re-dependent Nu number increased with higher volume fraction and the slope more pronounced at higher Re number for 2% volume [3]. Furthermore, others had investigated the nanofluid using two-phase approach but no comparison was made with the single-phase model [4]-[6]. In modeling the two phase flow, the nanoparticle equation velocity used is still in doubt. Since the direct measurement of the nanoparticle velocity is hardly measured, predicted nanoparticle velocity model become unclear. In this paper, the generality of the nanoparticle velocity equation is investigated for a range of different Reynolds number and nanoparticle volume fraction.

II. PHYSICAL MODEL DESCRIPTION

A. Model Details

In this paper, a two-dimensional wide microchannel is used as validation purposes and all detail of the microchannel is best described by Kalteh M. et al. [7].

B. Single Phase Model Governing Equations

The governing equations for mass, momentum, and energy for the whole domains of the MCHS are shown here as[8]:

1) Continuity Equations for the Coolant

$$\frac{\partial u}{\partial x}+\frac{\partial v}{\partial y}+\frac{\partial w}{\partial z}=0 \quad (1)$$

2) Momentum Equation

$$\rho_{nf}\left(\frac{\partial(uu)}{\partial x}+\frac{\partial(uv)}{\partial y}+\frac{\partial(uw)}{\partial z}\right)= \quad (2a)$$
$$-\frac{\partial p}{\partial x}+\mu_{nf}\left(\frac{\partial}{\partial x}\left(\frac{\partial u}{\partial x}\right)+\frac{\partial}{\partial y}\left(\frac{\partial u}{\partial y}\right)+\frac{\partial}{\partial z}\left(\frac{\partial u}{\partial z}\right)\right)$$

$$\rho_{nf}\left(\frac{\partial(uv)}{\partial x}+\frac{\partial(vv)}{\partial y}+\frac{\partial(vw)}{\partial z}\right)= \quad (2b)$$
$$-\frac{\partial p}{\partial x}+\mu_{nf}\left(\frac{\partial}{\partial x}\left(\frac{\partial v}{\partial x}\right)+\frac{\partial}{\partial y}\left(\frac{\partial v}{\partial y}\right)+\frac{\partial}{\partial z}\left(\frac{\partial v}{\partial z}\right)\right)$$

$$\rho_{nf}\left(\frac{\partial(uw)}{\partial x}+\frac{\partial(wv)}{\partial y}+\frac{\partial(ww)}{\partial z}\right)= \quad (2c)$$
$$-\frac{\partial p}{\partial x}+\mu_{nf}\left(\frac{\partial}{\partial x}\left(\frac{\partial w}{\partial x}\right)+\frac{\partial}{\partial y}\left(\frac{\partial w}{\partial y}\right)+\frac{\partial}{\partial z}\left(\frac{\partial w}{\partial z}\right)\right)$$

3) Energy Equation in Fluid Domain is shown as

$$\rho_{nf}C_{p,nf}\left(u\frac{\partial T_f}{\partial x}\right)+\left(v\frac{\partial T_f}{\partial y}\right)+\left(w\frac{\partial T_f}{\partial z}\right)= \quad (3)$$
$$k_{nf}\left(u\frac{\partial^2 T_f}{\partial x^2}\right)+\left(v\frac{\partial^2 T_f}{\partial y^2}\right)+\left(w\frac{\partial^2 T_f}{\partial z^2}\right)$$

and for solid domain is written as:

$$k_s\left(u\frac{\partial^2 T_s}{\partial x^2}\right)+\left(v\frac{\partial^2 T_s}{\partial y^2}\right)+\left(w\frac{\partial^2 T_s}{\partial z^2}\right)=0 \quad (4)$$

C. Two-Phase Model Governing Equations

In mixture model, FLUENT solves the continuity equation for the mixture, the momentum equation for the mixture, the energy equation for the mixture, and the volume fraction equation for the secondary phases.

1) Continuity Equations for the Coolant

$$\frac{\partial}{\partial t}(\rho_m)+\nabla.(\rho_m\vec{v}_m)=\dot{m} \quad (5)$$

$$\vec{v}_m=\frac{\sum_{k=1}^{n}\phi_k\rho_k\vec{v}_k}{\rho_m} \quad (6)$$

$$\rho_m=\sum_{k=1}^{n}\phi_k\rho_k \quad (7)$$

where $\dot{m}$ = mass source, $\vec{v}_m$= mass-averaged velocity, ρ_m= mixture density, and α_k=volume fraction of the phase *k*.

2) Momentum Equation for the Coolant

$$\frac{\partial}{\partial t}(\rho_m\vec{v}_m)+\nabla.(\rho_m\vec{v}_m)=-\nabla p+\nabla.[\mu_m(\nabla\vec{v}_m \quad (8)$$
$$+\nabla\vec{v}_m^{T})]+\rho_m\vec{g}+\vec{F}+\nabla.\left(\sum_{k=1}^{n}\phi_k\rho_k\vec{v}_{dr,k}\right)$$

$$\mu_m=\sum_{k=1}^{n}\phi_k\mu_k \quad (9)$$

and $\vec{v}_{dr,k}=\vec{v}_k-\vec{v}_m$ (10)

where n = number of phases, $\vec{F}$ = is a body force, μ_m= the viscosity of the coolant, $\vec{v}_{dr,k}$=drift velocity for secondary phase, *k*

3) Energy Equation in Fluid Domain is shown as

$$\frac{\partial}{\partial t}\sum_{k=1}^{n}(\phi_k\rho_k E_k)+\nabla.\sum_{k=1}^{n}(\phi_k\vec{v}_k(\rho_k E_k+p)) \quad (11)$$
$$=-\nabla.(k_{eff}\nabla T)+S_E$$

$$E_k=h_k-\frac{p}{\rho_k}+\frac{v_k^2}{2} \quad (12)$$

where E_k= h_k(incompressible phase)=sensible enthalpy for phase *k*.

4) Relative (slip) Velocity and the Drift Velocity are

$$\vec{v}_{pq}=\vec{v}_p-\vec{v}_q \quad (13)$$

$$\vec{v}_{dr,p}=\vec{v}_{pq}-\frac{\sum_{k=1}^{n}\phi_k\rho_k}{\rho_m}\vec{v}_{qk} \quad (14)$$

$$\vec{v}_{pq}=\frac{(\rho_p-\rho_m)d_p^2}{18\mu_q f_{drag}}\vec{a} \quad (15)$$

with d_p= particle diameter, $\vec{a}$ = secondary phase particle's acceleration.

The drag function f_{drag} is taken from Schiller and Naumann where;

$$f_{drag}=\{1+0.15\,\mathrm{Re}^{0.687} \quad \mathrm{Re}\le 1000 \quad (16)$$

$$f_{drag}=\{0.0183 \quad \mathrm{Re}>1000 \quad (17)$$

where

$$\vec{a}=\vec{g}-(\vec{v}_m.\nabla)\vec{v}_m-\frac{\partial\vec{v}_m}{\partial t} \quad (18)$$

5) Volume Fraction Equation for Secondary Phases

$$\frac{\partial}{\partial t}(\phi_p\rho_p)+\nabla.(\phi_p\rho_p\vec{v}_m)=-\nabla.(\phi_p\rho_p\vec{v}_{dr,p}) \quad (19)$$

D. Boundary Conditions

The boundary conditions are being specified from Kalteh M. et al. [7]. The transverse velocity is assumed to be zero (u_z=0), and the inlet velocity is calculated as:

$$u_{in}=\frac{\mathrm{Re}\,\mu}{\rho D_h} \quad (20)$$

$$U=\frac{u}{u_{in}} \quad (21)$$

The uniform heat flux of 20.5 kW/ m^2 is applied at the bottom of the heat sink with 0.6 to 3.4 gs^{-1} mass flow rate at the inlet. The boundary conditions in the model are being set up as these:

1) Linear Velocity at the Inlet

$$u_{x=0} = u_{in}, \quad v_{x=0} = 0, \quad w_{x=0} = 0, \quad T_{x=0} = T_0 \tag{22}$$

2) Atmospheric Pressure at the Outlet

$$p_{x=0} = p_{out} \tag{23}$$

3) Fluid-Solid Interface

$$u = v = w = 0, \quad T_f = T_s, \quad -k_{eff}\frac{\partial T_{nf}}{\partial n} = -k_s\frac{\partial T_s}{\partial n} \tag{24}$$

4) Top Wall of the Heat Sink; and

$$q_w = -k_s\frac{\partial T_s}{\partial n} \tag{25}$$

5) Other Wall and Symmetric Wall

$$\frac{\partial T_s}{\partial n} = 0 \tag{26}$$

and the heat transfer coefficient is written as:

$$h = \frac{q^{"}}{\Delta T} = \frac{q^{"}}{T_{side} - T_{bulk}} \tag{27}$$

The other practical interest of heat transfer performance is shown by non-dimensionless Nu number, which is calculated using equation:

$$Nu = h\frac{D}{k} \tag{28}$$

E. Thermophysical Properties

Both fluid and solid properties are assumed to be constant. The constant β for Al_2O_3, CuO and SiO_2 are taken directly from a curve-fit relations [9], [10]. The general applied model for nanofluid properties are shown in this section.

1) Density

$$\rho_{nf} = (1-\theta)\rho_f + \theta\rho_{np} \tag{29}$$

2) Specific Heat [11]

$$(\rho Cp)_{nf} = (1-\theta)(\rho Cp)_f + \theta(\rho Cp)_{np} \tag{30}$$

3) Thermal Expansion Coefficient

$$(\rho\beta)_{nf} = (1-\theta)(\rho\beta)_f + \theta(\rho\beta)_{np} \tag{31}$$

4) Viscosity

$$\mu_{nf} = \frac{\mu_f}{1 - 34.87\left(\frac{d_p}{d_f}\right)^{-0.3}\varphi^{1.03}} \tag{32}$$

where $d_f = \frac{6M}{N\pi\rho_{f0}}$ (33)

5) Thermal Conductivity

$$k_{nf} = k_{static} + k_{Brownian} \tag{34}$$

$$k_{static} = k_f\left[\frac{(k_{np}+2k_f) - 2\phi(k_f - k_{np})}{(k_{np}+2k_f) - \phi(k_f - k_{np})}\right] \tag{35}$$

$$k_{Brownian} = 5x10^4\beta\phi\rho_f C_{p,f}\sqrt{\frac{\kappa T}{2\rho_{nf}R_{np}}}f(T,\phi) \tag{36}$$

where κ=1.3807x10^{-23} J/K and β is the fraction of the liquid volume which travels with a particle, while

$$f(T,\phi) = (2.8217\,x\,10^{-2}\phi + 3.917\,x\,10^{-3})\left(\frac{T+273.15}{T_0+273.15}\right) + (-3.0669\,x\,10^{-2}\phi - 3.91123\,x\,10^{-3}) \tag{37}$$

In this paper, three different nanoparticle velocity equations had been applied as listed in (38)-(40).

$$u_p = \frac{2k_BT}{\pi\mu_{pw}d_{np}^2} \quad [7], [12] \tag{38}$$

$$u_p = \frac{k_BT}{3\pi\mu_{pw}d_{np}l_{pw}} \quad [13] \tag{39}$$

$$u_p = \frac{1}{d_{np}}\sqrt{\frac{18k_BT}{\pi\rho d_{np}}} \quad [14], [15] \tag{40}$$

III. Numerical Modeling

The fluid flow and heat transfer is modeled by employing the finite volume method at which both fluid and solid domain are included. The whole domain is then separated using grids and meshes for computational purposes that varied according to the work by Kalteh M. et al. [7] for extensive accuracy and minimum deviation.

The physical models and the boundary conditions are then defined. All the governing equations are solved iteratively as a steady-state flow. The partial differential equations are being evaluated using Finite Volume Method (FVM) and calculated at each of the meshed geometry. The standard SIMPLEC algorithm is used to solve the pressure equation. The second order upwind scheme is used for both the momentum and energy conservation equations. To improve the convergence, the residual levels are lowered to 10^{-6} and 10^{-9} for velocities and energy equation while the fluxes are below 1%.

In the mixture model, both phases are modeled as fluid to represent a continuum fluid. Two different drag coefficient models are applied, named as Schiller and Naumann model and Morsi and Alexander model. The first model specifies the flow for Re ≤ 1000 and Re > 1000. Meanwhile, the second model is more complete with various range of Reynolds number condition. For run1 at Reynolds number of 67.41,

both models are acceptable since no change in value is observed for the Nusselt number.

The value taken using either area-weighted average or mass-weighted average may lead to deviation. In this paper, the heat flux and the wall temperature is taken as area-weighted average value while the bulk temperature is predicted as mass-weighted average value.

IV. Results and Discussion

A. Thermal Performance

In order to investigate the validity of present numerical work on nanofluid, the validation work is performed with the work of Kalteh M. et al. [7] inside a wide rectangular microchannel. The deviation in between experimental data and numerical work for pure water coolant is in the range of 0.24 to 4.29% as shown in Fig. 1.

As the fluid flows inside the channel, different velocity is predicted and accelerates along the entrance while the boundary layer is being developed as in Fig. 3. The accelerated bulk velocity soon vanishes as the growth of boundary layer meets each other. After this point, the bulk velocity flows constantly until the end of the channel and the flow reaches the fully developed flow. As the Reynolds number increases, the entry length increases before it reaches the fully developed condition. Also shown is that the length represented by accelerated bulk velocity in x-axis as displayed become longer as the Reynolds number increases from 67.41 to 286.77. This delay the merge of boundary layer and the layer becomes thinner that finally causes lower difference temperature of the wall and the bulk fluid. This finally helps in promoting higher heat transfer.

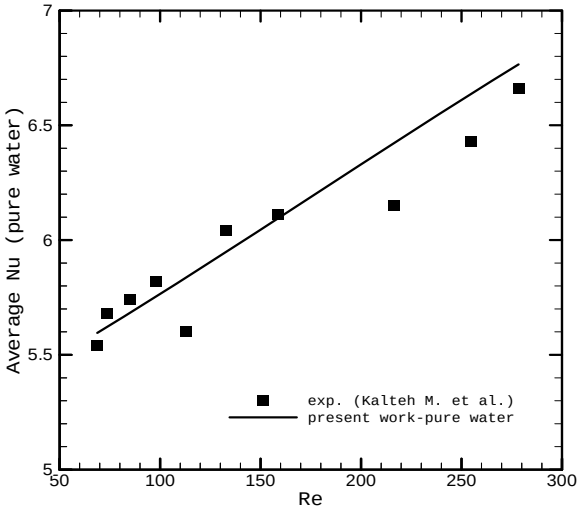

Fig. 1 Average Nusselt number for pure water

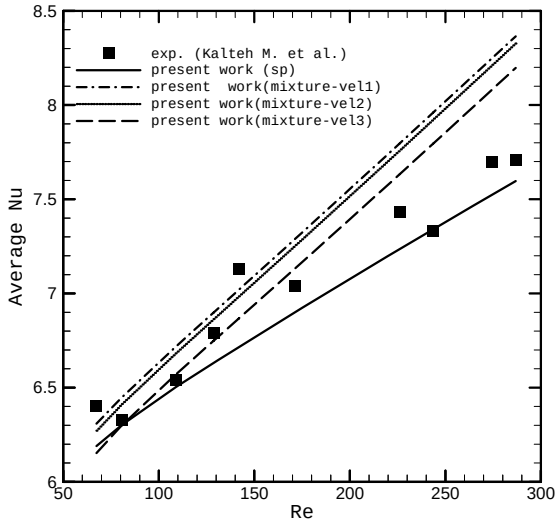

Fig. 2 Average Nusselt number for 0.1% volume fraction of alumina

Higher heat transfer coefficient also leads to higher percentage in Nusselt number increment with highest percentage of 25 to 28% at Reynolds number of 168 as in Fig. 4. At Reynolds number higher than this value, the increment in Nusselt number is predicted to decrease to 25% which explains slower percentage of Nusselt number increment. This can be shown too with higher ratio of T_w-T_b for pure water to nanofluid as in Fig. 5. This pattern shows the favorable of using nanofluid at lower Reynolds number. However, the superior of using nanofluid instead of water is still an advanced. Furthermore, the Nusselt number increment pattern agrees well with the experimental value. Underpredicted Nusselt number increment is observed for single phase approach while overpredicted values for two-phase approach.

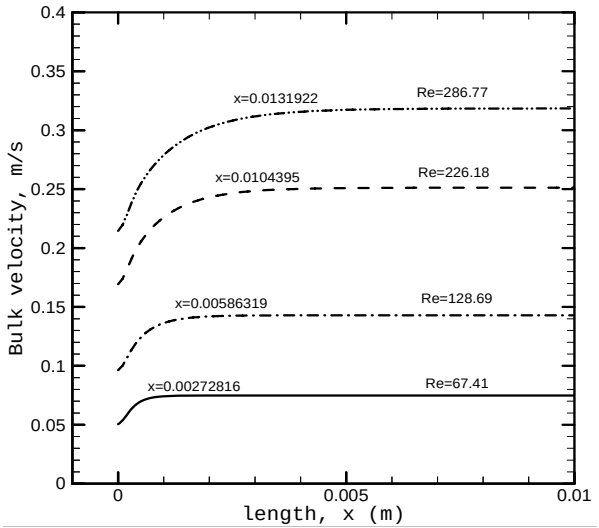

Fig. 3 Bulk velocity along the channel at various Reynolds number

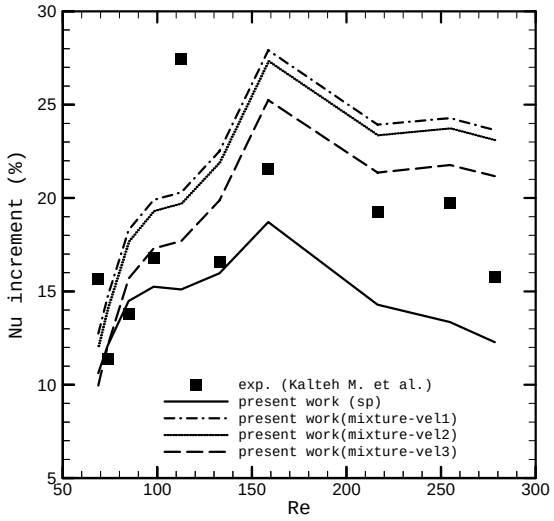

Fig. 4 Increment of average Nusselt number for 0.1% volume fraction of alumina

For single phase model, the nanofluid is assumed to be continuum and the constitution of nanofluid in terms of atom is disregard. This is based on Knudsen number that identifies the flow regime. In this study, the Knudsen number less than unity shows that the single-phase model is still appropriate for modeling nanofluid in the microchannel. The properties of the mixture are taking as intermediate property between the property of the base fluid and nanoparticles. The prediction of nanofluid using single phase model is underpredicted the heat transfer augmentation. This is because the thermal conductivity augmentations of the nanofluid that attribute to the overall heat transfer increment are highly influenced by the nanoparticle itself which is not being modeled in molecular state.

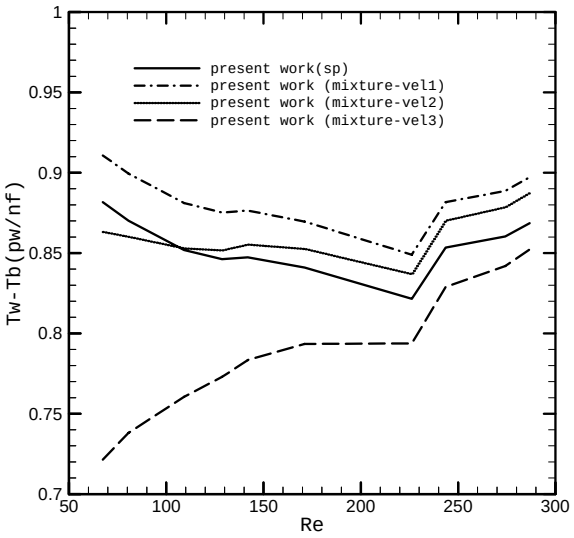

Fig. 5 Ratio of T_{wall}-T_{bulk} of pure water to nanofluid

For the two-phase model, both water and nanoparticles are also considered as continuum and treated as penetrated continua. The slip velocity in between the phases is being considered compared to single phase model. The interfacial heat transfer and the lift forces are accounted through this model.

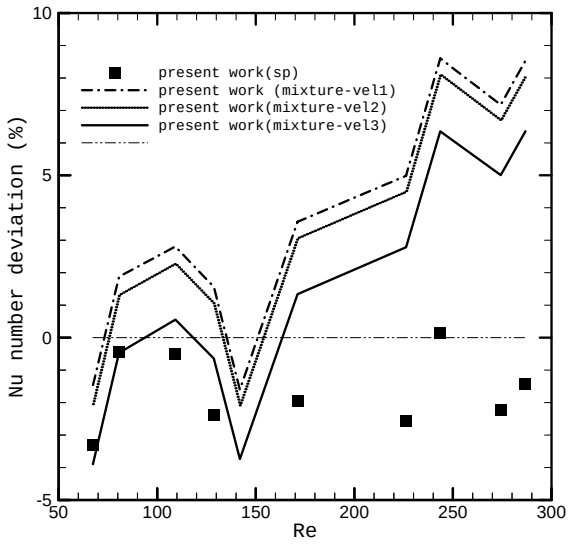

Fig. 6 Deviation of the Nusselt number at various Reynolds number

The single phase model shows very small deviation to the experimental value at which most value underpredicted the Nusselt number in between 0.15 to 5.86%. For two phase model, the range of deviation is fluctuating under and overpredicted within -3.90% to 8.36%. For two phase models, increasing deviation are noticed at higher Reynolds number and very close to experimental value at 80<Re<130. However, all model lies in acceptable range with less than 10%. At Reynolds number of 128.7, all nanoparticle velocity value gives very close result of Nusselt number with deviation up to 0.05% with the experimental value as shown in Fig. 6.

Greater deviations are predicted as Reynolds number increase. At Reynolds number higher than 170, the average Nusselt number increase correspondingly with the rise of the Reynolds number. Tremendous increment in Nusselt number is measured and predicted at Re<100 and monotonous decrement afterwards is observed.

As the volume concentration of nanoparticle increases from 0.01 to 0.4%, the two-phase model predicted increment in average Nusselt number as shown in Fig. 7. Monotonous increment is observed using (38) and (39) while drastic increment is noted using (40).

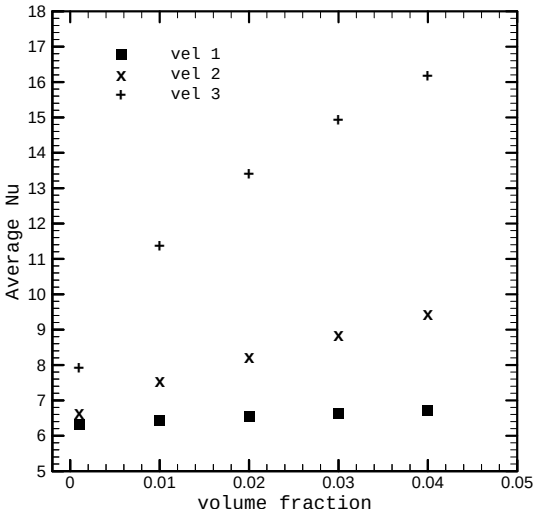

Fig. 7 Average Nusselt number at Reynolds number=300 and dp=100nm for various nanoparticle volume fraction

B. Generality of Nanoparticle Velocity

The generality of the nanoparticle velocity is still in doubt since no exist equation is appropriate for extensive range of application especially for nanofluid. In this paper, three different nanoparticle velocities from published paper are taken into account for a wide range experimental and numerical application including various Reynolds number and nanoparticle volume fraction. The evaluation of the heat transfer in terms of the Nusselt number enhancement is then being compared. The velocity using (40) shows the closest one with experimental data.

The root mean square velocity is defined from root mean square displacement in (41).

$$x_{rms} = \sqrt{2DT} \tag{41}$$

with D is the diffusion coefficient. This is based on kinetic theory of gases at which the average of particles moving freely without interacting each other through the Maxwell-Boltzmann distribution.

The diffusivity equation is derived from Stokes-Einstein formula and is interrelated with the Brownian motion velocity. The diffusion coefficient explains the ratio of kinetic to the viscous effect and relates the viscosity of heavy Brownian particle in a liquid medium. The diffusion occurs due to the fluctuation of molecules velocity due to different gradient in concentration, temperature or even mean velocity. The Stokes-Einstein formula is originated from Albert Einstein's work in 1905 and had been extended by later researchers to model the flow of nanofluid. The Stokes-Einstein equation explains the macroscopic spherical-shape particle diffusivity in a liquid medium. The particle diffusivity is viscosity, temperature and particle size dependent and defined as

$$D = \frac{k_B T}{C \pi \mu_{pw} r_{np}} \tag{41}$$

at which C is the constant. However, the Stokes-Einstein formula is limited to very dilute solution, at which the nanoparticles concentration is too low and low Reynolds number near zero. The limitation of this equation also holds for the case where there is no slip in between the nanoparticle and the pure water, which is the assumption of single phase nanofluid.

By using (38) to (40), the Brownian velocity of nanoparticles differs according to the terms defined by previous work. These include the mean free path of nanofluid particle and the constant used in diffusion coefficient equation as in (41). In (38), the mean free path is assumed to be equal to the radius of the particle. Meanwhile in (39), the velocity of the solid particle is assumed to flow across the base fluid molecule. However, the mean free path of the base fluid is based on the ideal gas calculation. Equation (40) is defined by Probstein [16] and also accounted for the distance traveled by the particle in one direction due to particle motion at which the speed varies between 1.63 - 1.63e^{-3} m/s for particle size of 10 - 1000 nm [3]. Due to macroscopic level and few assumptions made before, the accuracy in using the nanoparticle velocity may cause some deviation and further study is very significant.

V. Conclusion

Numerical simulations on the fluid flow and heat transfer characteristics in single rectangular interrupted microchannel heat sink were carried out. The generality of Brownian motion velocity is investigated in various Reynolds number and nanoparticle volume concentration. The following conclusions can be withdrawn as:

1) The average Nusselt number of all model increase with the increase in Reynolds number.
2) Thinner boundary layer is expected with increasing in entry length as Reynolds number increases.
3) There exists an optimal Reynolds number at which the average Nusselt number increment compared to pure water is maximized at Reynolds number of 168 with highest percentage of 25 to 28%.
4) Smaller deviation of Nusselt number with experimental data using single phase model compared to two phase model with underpredicted value in between 0.15 to 5.86%.
5) For two phase model, the range of deviation is fluctuating under and overpredicted within -3.90% to 8.36%.
6) Nanoparticle velocity equation using (40) shows very close prediction with experimental data compared with other equations.

References

[1] Akbari, M., N. Galanis, and A. Behzadmehr, Comparative analysis of single and two-phase models for CFD studies of nanofluid heat transfer. *International Journal of Thermal Sciences,* 2011. 50: p. 1343-1354.

[2] Kalteh, M., et al., Eulerian-Eulerian two-phase numerical simulation of nanofluid laminar forced convection in a microchannel. *International Journal of Heat and Fluid Flow,* 2011. 32(1): p. 107-116.
[3] Chein, R. and G. Huang., Analysis of microchannel heat sink performance using nanofluids. *Applied Thermal Engineering*, 2005. 25(17-18): p. 3104-3114.
[4] Alinia, M., D.D. Ganji, and M. Gorji-Bandpy, Numerical study of mixed convection in an inclined two sided lid driven cavity filled with nanofluid using two-phase mixture model. *International Communications in Heat and Mass Transfer*, 2011. 38(10): p. 1428-1435.
[5] Mirmasoumi, S. and A. Behzadmehr., Numerical study of laminar mixed convection of a nanofluid in a horizontal tube using two-phase mixture model. *Applied Thermal Engineering*, 2008. 28(7): p. 717-727.
[6] Shariat, M., et al., Numerical study of two phase laminar mixed convection nanofluid in elliptic ducts. *Applied Thermal Engineering*, 2011. 31(14-15): p. 2348-2359.
[7] Kalteh, M., et al., Experimental and numerical investigation of nanofluid forced convection inside a wide microchannel heat sink. *Applied Thermal Engineering* 2012. 36: p. 260-268.
[8] Patankar, S.V., *Numerical Heat Transfer and Fluid Flow*. 1980, New York: Hemisphere Publishing Corporation.
[9] Sahoo, B.C., Measurement of Rheological and Thermal Properties and the Freeze-Thaw Characteristics of Nanofluids. 2008: University of Alaska Fairbanks.
[10] Vajjha, R.S. and D.K. Das, Measurement of thermal conductivity of three nanofluids and development of new correlations. *Int. J. Heat Mass Transfer*, 2009. 52: p. 4675-4682.
[11] Xuan, Y. and W. Roetzel, Conceptions for heat transfer correlation of nanofluids. *Int. J. Heat Mass Transfer*, 2000. 43(19): p. 3701-3707.
[12] Patel, H.E., et al., A micro-convection model for thermal conductivity of nanofuids. *Journal of Physics*, 2005. 65(5): p. 863-869.
[13] Jang, S.P. and S.U.S. Choi, Role of Brownian motion in the enhanced thermal conductivity of nanofluids. *Appl. Phys. Lett*, 2004. 84.
[14] Koo, J. and C. Kleinstreuer, A new thermal conductivity model for nanofluids. *Journal of Nanoparticle Research*, 2004. 6(6): p. 577-588.
[15] Prasher, R., P. Bhattacharya, and P.E. Phelan, Brownian-Motion-Based Convective-Conductive Model for the Effective Thermal Conductivity of Nanofluids. *Journal of Heat Transfer*, 2006. 128: p. 588-595.
[16] Probstein, R.F., *Physicochemical Hydrodynamics-A Introduction*. 2003: A Wiley-Interscience Publication, John Wiley & Sons, INC.